의학박사 학위논문

Expression of Class III Beta-Tubulin is Associated with Invasive Potential and Poor Prognosis in Thyroid Carcinoma

갑상선암에서 class III 베타 튜불린이 종양의 침습성과 예후에 끼치는 영향

2021년 8월

서울대학교 대학원

의학과 병리학 전공

나 희 영

갑상선암에서
Class III 베타 튜불린이
종양의 침습성과 예후에 끼치는 영향

지도교수 김 지 은

이 논문을 의학박사 학위논문으로 제출함

2021년 6월

서울대학교 대학원

의학과 병리학 전공

나 희 영

나 희 영 의 의학박사 학위논문을 인준함

2021년 6월

위 원 장 정경화

부 위 원 장 김 지 은

위 원 박 영 주

위 원 김 영 아

위 원 윤 선 옥

Expression of class III beta-tubulin is associated with invasive potential and poor prognosis in thyroid cancer

by

Hee Young Na

A thesis submitted to the Department of Medicine in partial fulfillment of the requirements for the Degree of Doctor of Philosophy in Medicine (Patholgoy) at Seoul National University College of Medicine

June 2021

Approved by Thesis Committe:

Professor Kyong Chem Jung Chairman

Professor Ji Eun Kim Vice chariman

Professor Young Joo Park

Professor Young A Kim

Professor Sun Och Yoon

Abstract

Thyroid cancer is one of the most common human malignancies worldwide. Due to the high-resolution ultrasonography-guided thyroid screening system, the incidence of thyroid cancer is continuously rising in Korea. Although most differentiated thyroid cancers are indolent, a subset of tumors show aggressive features, including local recurrences or distant metastasis, which have led many researchers to excavate novel prognostic factors in thyroid cancer. Although American Thyroid Association guidelines offer risk stratification scheme for thyroid cancer patients, there is a continuous need for more sophisticated biomarkers. In this study, we aimed to evaluate the prognostic value of class III beta-tubulin (TUBB3) and uncover the relationship between TUBB3 and invasive potential and epithelial-mesenchymal transition (EMT) in thyroid carcinoma.

Tissue microarray construction and immunohistochemistry (IHC) for TUBB3 and E-cadherin (ECAD) was performed in a total of 254 cases of thyroid cancer specimens, including 123 conventional papillary carcinomas (cPTCs), 11 infiltrative follicular variant papillary carcinomas (FVPTCs), 84 invasive encapsulated FVPTCs (invEFVPTCs), 25 non-invasive follicular thyroid neoplasm with papillary-like nuclear features (NIFTPs), and 11 anaplastic thyroid carcinomas (ATCs). To find a link with epithelial mesenchymal transition, tumor budding at the invasive margin

was evaluated. In vitro functional studies were also performed; the protein and mRNA levels of TUBB3 were compared among the five cell types including normal follicular cells (Htori-3), cPTC cells (BCPAP), FVPTC cells (MDA-T68), and ATC cells (BHT101 and 8505C), at baseline, with transwell invasion, and after blocking of TUBB3 by shRNA.

IHC revealed that the levels of TUBB3 expression were significantly higher in cPTCs and ATCs than in infiltrative FVPTCs, invEFVPTCs, and NIFTPs, whereas ECAD expression showed a reversal trend. In cPTC, higher tumoral TUBB3 expression was associated with frequent tumor budding. In vitro cell line study revealed highest TUBB3 protein and mRNA expression levels in ATC cells at baseline. In transwell invasion assay, only ATC cells invaded to bottom chamber through matrigel. After blocking of TUBB3 with shRNA transfection, the protein and mRNA expression level of TUBB3 decreased and fewer cells invaded to bottom chamber. In univariate survival analysis, high tumor budding and tumoral TUBB3 expression were associated with inferior progression-free survival in cPTC. Data from The Cancer Genome Atlas database showed that TUBB3 mRNA expression level was highest in tall cell variant PTCs, followed by cPTCs and FVPTCs. EMT score, which was calculated from mRNA expression level of 16 EMT-associated gene markers, correlated with TUBB3 mRNA expresseion level.

Our results suggest that high expression of TUBB3 in thyroid carcinoma could predict invasive potential and possibly

be linked with EMT. TUBB3 could be a novel prognostic marker in cPTC.

Keyword : Thyroid carcinoma, Class III beta-tubulin, Invasion, Epithelial-mesenchymal transition, Prognosis
Student Number : 2014-21977

Table of Contents

List of Tables

List of Figures

Introduction

Study Background

Thyroid cancer is one of the most common human malignancies with a steadily rising incidence worldwide. Due to the overall indolent behavior of this tumor, there have been controversies over managing all patients with radical treatment, including lymph node dissection [1, 2]. Concerns about overdiagnosis and overtreatment have led to the concept of "active surveillance" in papillary microcarcinoma (PMC) [3-5]. However, despite a 5-year survival rate of nearly 100%, a minority of papillary thyroid carcinomas (PTCs), including aggressive histologic variants and even PMCs, may develop distant metastasis or local recurrence during the follow-up period, which severely affects patients' quality of life [6-10]. This implies a biologic diversity of thyroid carcinoma, requiring more precise stratification to identify the subgroup that needs aggressive management and meticulous study. Because AJCC/TNM staging is focused on predicting the risk of death, various other systems, such as EORTC, AGES and AMES have been developed to assess the risk of recurrence [11-14], although no one system has shown superiority over the others. The 2015 American Thyroid Association (ATA) guidelines proposed an updated risk stratification system modified from the 3-tiered 2009 system, combining additional factors including the extent of lymph node involvement and mutational status [15, 16]. However, even this updated scheme requires further

validation and there is still an increasing demand for a new reliable biomarker.

Class III beta-tubulin (TUBB3) is one of nine beta-tubulin isoforms; it forms a heterodimer with alpha-tubulin and participates in building up microtubules, which play a role in maintaining cell shape, intracellular transport and chromosome separation during mitosis and meiosis [17]. Traditionally, TUBB3 is known to be expressed exclusively in terminally differentiated neuronal tissue and testis [18, 19]. However, TUBB3 gained its clinical significance as researchers confirmed the association between TUBB3 expression in epithelial tumors, including ovary, lung, and breast cancer, with resistance to Taxol-based chemotherapy [20-23]. In addition, TUBB3 expression has been proven to be associated with aggressive features independent of chemotherapy status in various cancers, including breast, lung, and colon cancer [24-30].

Epithelial-mesenchymal transition (EMT) is a dynamic cellular process in which epithelial cells acquire mesenchymal phenotype [31]. EMT occurs in both non-neoplastic and neoplastic circumstances; Embryonic development, tissue regeneration, and wound healing are typical examples of non-neoplastic cases [32]. In cancer, tumor cells gain the ability to migrate and metastasize through EMT [32]. Some researchers have suggested a relationship of TUBB3 with EMT revealing a positive correlation between TUBB3 and some EMT markers, such as Snail [40]. This link has been more strongly suggested by Zhao et al. who demonstrated a positive correlation between TUBB3 and lymph node metastasis in colorectal carcinoma [30].

Tumor budding, defined as a single cell or a cluster of less than 5 cells in fibrotic stroma, is reported in various cancers [33-35] and has been intensively studied in colorectal cancer [36]. Researchers have demonstrated reduced E-cadherin [34, 37] and increased vimentin expression [37] in tumor budding, and thus tumor budding was thought to be EMT-related phenomenon. Also, tumor budding was associated with clinical parameters such as lymph node metastasis, or disease progression [38, 39]. There have been few reports about the link between TUBB3, and tumor budding, but Portyanko et al. demonstrated higher TUBB3 expression at the tumor budding in colorectal adecarcinoma[28].

In thyroid cancer, TUBB3 has been scarcely studied [41-43]. Colato et al. have demonstrated virtually absent TUBB3 expression in normal follicular cells, nodular hyperplasia, and follicular thyroid adenomas [41, 42]. They reported strong TUBB3 expression in the invasive front of PTCs which show infiltrative growth pattern, such as conventional PTCs (cPTCs) [41, 42]. On the contrary, PTCs with well demarcated margin generally showed low TUBB3 expression [41, 42]. Another previous study investigated TUBB3 expression in various PTC variants and found out that high TUBB3 expression was more common in aggressive histologic variants [43].

Recently, an international mutlidiciplinary collaborative group proposed a new diagnostic terminology, "noninvasive follicular thyroid neoplasm with papillary-like nuclear feature (NIFTP)", for a specific subset of encapsulated/noninvasive follicular variant PTCs, due to an extremely indolent disease course [45]. Although one should apply a set of strict diagnostic

criteria, diagnosing NIFTP can prevent the overtreatment and decrease medical expenses in patients.

Purpose of Research

To date, there have been few studies exploring the role of TUBB3 and tumor budding in thyroid cancer [41-44]. In this study, we comprehensively investigated the expression of TUBB3 in various types of thyroid carcinomas, including the newly emerging entity, NIFTP. We aimed to evaluate the clinicopathologic significance of TUBB3 and tumor budding in relation to EMT in thyroid carcinoma.

Materials and methods

Patients and samples

Samples of thyroid carcinoma were obtained from patients who received thyroidectomy at Seoul National University Hospital and Seoul National University Boramae Hospital from 1992 to 2013. Histopathologic diagnoses, including tumor type and variant, were confirmed by three experienced pathologists (HYN, JEK, and JKW), according to the 2017 WHO classification [46]. The number of tumor budding, which was defined as the presence of isolated cells or clusters composed of fewer than 5 cells in the stroma at the invasive margin [36], was counted in PTCs and NIFTPs. Clinical and pathological data were obtained from electronic medical records. This study was approved by the Institutional Review Board of Seoul National University Boramae Hospital (IRB No. 26-2017-44).

Immunohistochemistry (IHC)

Tissue microarray blocks were constructed with a pair of 3-mm wide core tissues, including both tumoral and peritumoral stromal areas from the most representative paraffin-embedded blocks. For cases with small tumor volumes, such as PMC, whole section slides were used for IHC. IHC using anti-TUBB3 (TUJ1, 1:200; Covance, Princeton, NJ, USA), anti-E-cadherin (ECAD) (HECD-1, 1:100; abcam, Cambridge, UK) antibodies and BRAF

mutation-specific antibody (VE1, 1:100; Spring Bioscience, Pleasanton, CA, USA) was performed according to the validated protocols using an automated immunostainer (Ventana, Tuscon, AZ, USA). Of these, BRAF IHC was performed only in cPTC. In tumoral area, the expression of TUBB3 was semiquantitatively estimated by using H-score modified from which Levallet et al. used [47]. H-score was calculated by multiplying 3-tiered intensity scores (0, absent; 1, weak; 2, moderate to strong) and the frequency scores (the percentage of positive tumor cells). In the peritumoral stroma, TUBB3 expression was interpreted as low (absence or focal weak positivity) or high (moderate to strong positivity). For ECAD, the percentage of tumor cells showing loss of ECAD was manually calculated. Finally, a case was considered positive for BRAF VE1 if it displayed moderate to strong staining intensity irrespective of the number of tumor cells stained [48].

Baseline levels of TUBB3 in thyroid cell lines

Human thyroid cell lines, including Htori-3 cells (normal thyroid follicular cells, kindly provided by Dr. YJ Park, Seoul National University Hospital), BCPAP cells (cPTC cells, a gift from Dr. YJ Park), MDA-T68 cells (follicular variant PTC (FVPTC) cells, purchased from ATCC, Manassas, VA, USA), BHT101 cells (anaplastic thyroid carcinoma (ATC) cells, provided by Dr. YJ Chae, Department of Surgery, Seoul National University Boramae hospital), and 8505C cells (ATC cells, a gift from Dr. YJ Chae), were used in the experiment. Protein

expression of TUBB3 and ECAD was checked by western blot and immunofluorescence (IF), and mRNA levels were investigated by reverse transcriptase PCR (RT-PCR). Western blotting was performed as previously described [49]. Briefly, a total of 30 μg of protein from each cell line was transferred to polyvinylidene difluoride membranes and incubated with primary antibodies against TUBB3 (TUJ1, 1:5000; BioLegend, San Diego, CA, USA), E-cadherin (HECD-1, 1:1000; Abcam, Cambridge, UK), vimentin (D21H3, 1:1000; Cell Signaling Technology, Beverly, MA, USA), and β-actin in TBST (TBS containing 0.05% Tween 20) at 4C overnight. After blocking and application of secondary antibodies, the bands were visualized using chemiluminescence. For IF, the cells were fixed with PBS containing 4% paraformaldehyde and incubated with the same primary antibodies as used in the western blot. A FITC IgG conjugate (Sigma Aldrich, St Louis, MO) was used as the secondary antibody, and the nuclei were counterstained with 4′,6′-diamino-2-phenylindole (DAPI). RT-PCR was performed using TRIzol reagent (Thermo Fisher Scientific, Waltham, MA, USA) for RNA extraction, and the QuantiTect Reverse Transcription Kit (Qiagen, Hilden, Germany) for cDNA construction. Amplification was conducted using the OneStep RT-PCR Kit (Qiagen). Specific primers targeting TUBB3 (amplifying a 353 bp fragment; forward, 5′-AAGCCGGGCATGAAGAAGT-3′ and reverse, 5′-AGCAAGGTGCGTGAGGAGTA-3′) The amplified PCR products were resolved by 2% agarose gel and stained with ethidium bromide.

Transwell invasion assay

Transwell chambers (Corning Incorporated, Corning, NY, USA) were used for the invasion assay. Approximately 1×10^5 cells from each cell line were isolated before being added to the upper chamber of a transwell coated with Matrigel. After incubation for 24 hours, the cells below the surface of the lower chamber were fixed with 4% paraformaldehyde solution and stained with Giemsa. The invading cells were observed in five different randomly selected fields under a microscope. Expression of TUBB3 was visualized by immunofluorescence (IF) using the same primary antibody under a fluorescence microscope (Axio Imager Z1, Zeiss, Germany). Cells that penetrated the Matrigel were collected and examined for the levels of TUBB3, ECAD, and vimentin by western blot and RT-PCR.

Blocking of TUBB3 by shRNA transfection

Lentivirus expressing shRNA against TUBB3 (Santa Cruz Technology, Santa Cruz, CA, USA) was transfected into ATC cells (BHT101 and 8505C) using Lipofectamine 2000 (Thermo Fisher Scientific). ATC cell lines were cultured for 24 hours, and 5 μg/ml shRNA was added to the cell lines. The cell lines without transfection were considered negative controls. Stable cell lines were selected with medium containing 2 μg/ml

puromycin for five more passages (12–15 days). The stable cell lines were harvested and validated with RT–PCR and western blot for further experiments.

Utilization of data from The Cancer Genome Atlas (TCGA)

We investigated the mRNA expression of TUBB3, ECAD, and vimentin as well as mutational profiles of TERT and BRAF gene in PTCs by using data extracted from cBioPortal for Cancer Genomics (http://www.cbioportal.org/index.do) in October 2019. A total of 493 cases of PTCs including 355 cPTCs, 102 FVPTCs (showing follicular pattern in ≥99% of tumor), and 36 tall cell variant PTCs (tall cell component in ≥50% of tumor) with the standardized level 3 RNA sequencing data and clinical data were included in the analyses. To investigate the association of TUBB3 mRNA expression with EMT, we calculated an EMT score by subtracting the RNAseq by expectation–maximization (RSEM) values of 3 epithelial marker genes (CDH1, DSP, and OCLN) from the sum of RSEM values of 13 mesenchymal marker genes (VIM, CDH2, FOXC2, SNAI1, SNAI2, TWIST1, FN1, ITGB6, MMP2, MMP3, MMP9, SOX10, and GCS) [50]. The RSEM values of TUBB3 were log2 (+1) transformed before analyzing the differences among PTC variants.

Statistical analysis

Spearman's ρ was used to assess the correlation between TUBB3 expression and other clinicopathologic variables. The Mann-Whitney U-test and Fisher's exact test were performed to compare TUBB3 expression and other clinicopathological parameters according to the subtypes of tumors. Corrections for multiple testing are performed with Bonferroni method and adjusted p-values are presented. Overall survival was calculated from the date of diagnosis to the date of death. Progression-free survival was calculated from the date of diagnosis to the date of local recurrence or the date of lymph node or distal metastasis after the date of diagnosis. Univariate Kaplan-Meier survival analyses with log-rank tests were performed to compare binary groups based on TUBB3 expression levels. Multivariate survival analysis using the Cox multiple regression model was performed to identify independent prognostic markers. The results were considered statistically significant with a two-tailed P-value of 0.05. All data were analyzed with SPSS software, version 22.0 (SPSS Inc., IBM, NY, USA).

Results

Patients

A total of 254 cases including 123 cPTCs, 11 infiltrative FVPTCs, 84 invasive encapsulated FVPTCs (invEFVPTCs), 25 NIFTPs, and 11 ATCs, were enrolled in this study. The clinicopathologic parameters are summarized in Table 1. There were 53 male and 201 female patients with a median age of 49 years (range 16 to 102). Regional lymph node metastasis at the time of diagnosis was found in 86 patients. During the follow-up period (median 170 months; range 0 to 300 months), disease progression, including death, local recurrence and distant metastasis, was observed in 32 patients.

Table 1. Clinicopathological parameters in different thyroid cancers

Parameters	cPTC (n=123)	infiltrative FVPTC (n=11)	invEFVPTC (n=84)	NIFTP (n=25)	ATC (n=11)	Total (n=254)
Sex						
Male, n (%)	21 (17.1)	0 (00.0)	20 (23.8)	9 (36.0)	3 (27.3)	53 (20.9)
Female, n (%)	102 (82.9)	11 (100.0)	64 (76.2)	16 (64.0)	8 (72.7)	201 (79.1)
Age (median, range) (years)	43 (16-102)	44 (24-63)	53 (26-73)	45 (26-71)	64 (54-77)	49 (16-102)
Tumor size (median, range)	2.1 (0.4-7.0)	2.0 (0.4-6.0)	1.7 (1.0-6.5)	1.9 (1.1-4.5)	4.0 (2.5-6.0)	2.0 (0.4-7.0)
Gross invasion, n (%)	25 (20.3)	0 (0.0)	0 (0.0)	0 (0.0)	3 (27.3)	28 (11.0)
LN metastasis, n (%)	63 (51.2)	4 (36.4)	16 (19.0)	0 (0.0)	3 (27.3)	86 (33.9)
Distant metastasis, n (%)	4 (3.3)	1 (9.1)	0 (0.0)	0 (0.0)	5 (45.5)	10 (3.9)
Stage						
I, n (%)	88 (71.5)	9 (81.8)	73 (86.9)	23 (92.0)	0 (0.0)	193 (76.0)
II-IV, n (%)	35 (28.5)	2 (12.2)	11 (13.1)	2 (8,0)	11 (100.0)	61 (24.0)
Death, n (%)	10 (8.1)	0 (0.0)	0 (0.0)	0 (0.0)	4 (36.4)	14 (5.5)
Disease progression, n (%)	26 (21.1)	1 (9.1)	0 (0.0)	0 (0.0)	5 (45.5)	32 (12.6)
OS (months, median, range)	229 (4-300)	199 (3-273)	49 (0-261)	46 (1-170)	7 (2-18)	170 (0-300)
PFS (months, median, range)	219 (4-300)	199 (3-273)	49 (0-261)	46 (1-170)	5 (1-18)	88 (0-300)

cPTC, conventional papillary thyroid carcinoma; FVPTC, follicular variant papillary thyroid carcinoma; invEFVPTC, invasive encapsulated follicular variant papillary thyroid carcinoma; NIFTP, non-invasive follicular thyroid neoplasm with papillary-like nuclear feature; ATC, anaplastic thyroid carcinoma; LN, lymph node; OS, overall survival; PFS, progression-free survival.

Differential expression of TUBB3 and ECAD in normal thyroid parenchyme and thyroid carcinomas

In non-neoplastic thyroid tissues, both follicular cells and stromal cells were negative for TUBB3 and positive for ECAD in a diffuse membranous pattern. In thyroid carcinoma, TUBB3 and ECAD showed different expression patterns according to histologic subtypes (**Table 2**). Expression of TUBB3 was diffuse and strong throughout the tumor area in ATCs. In cPTCs and infiltrative FVPTCs, TUBB3 was selectively expressed in the tumor and stromal cells at the invasive margin, forming a band-like structure. However, invEFVPTCs and NIFTPs showed only a few scattered positive cells (**Figure 1**). ATCs revealed the highest levels of TUBB3, followed by cPTCs, infiltrative FVPTCs, invEFVPTCs and NIFTPs, both in tumor cells and stromal cells, although the differences between ATCs and cPTCs were not statistically significant (**Table 3**). In contrast, the expression of ECAD showed the opposite pattern to that of TUBB3 (**Table 2-3, Figure 1, Figure 2**).

Table 2. Differential expression of TUBB3 and E-cadherin, and tumor budding among thyroid cancer.

Parameters	cPTC (n=123)	infiltrative FVPTC (n=11)	invEFVPTC (n=84)	NIFTP (n=25)	ATC (n=11)
Tumoral TUBB3 H-score					
Median (range)	90.0 (0.0-190.0)	5.0 (0.0-190.0)	1.0 (0.0-180.0)	1.0 (0.0-30.0)	120.0 (5.0-190.0)
Stromal TUBB3					
Low, n (%)	20 (16.3)	3 (27.3)	43 (51.2)	22 (88.0)	88 (34.6)
High, n (%)	103 (83.7)	8 (72.7)	41 (48.8)	3 (12.0)	166 (65.4)
E-cadherin loss (%)					
Median (range)	6.0 (0.0-100.0)	5.0 (0.0-20.0)	0.0 (0.0-10.0)	0.0 (0.0-5.0)	90.0 (10.0-100.0)
Tumor budding					
Present, n (%)	97 (78.9)	6 (54.4)	17 (20.2)	0 (0.0)	NA
Absent, n (%)	26 (21.1)	5 (45.5)	67 (79.8)	25 (100.0)	NA
Number of tumor budding					
Median (range)	1.5 (0.0-20.0)	3.0 (0.0-6.0)	0.0 (0.0-5.0)	0.0 (0.0-0.0)	NA

cPTC, conventional papillary thyroid carcinoma; FVPTC, follicular variant papillary thyroid carcinoma; invEFVPTC, invasive encapsulated follicular variant papillary thyroid carcinoma; NIFTP, non-invasive follicular thyroid neoplasm with papillary-like nuclear feature; ATC, anaplastic thyroid carcinoma; NA, not applicable.

Figure 1. TUBB3 and E-cadherin expression in thyroid cancers

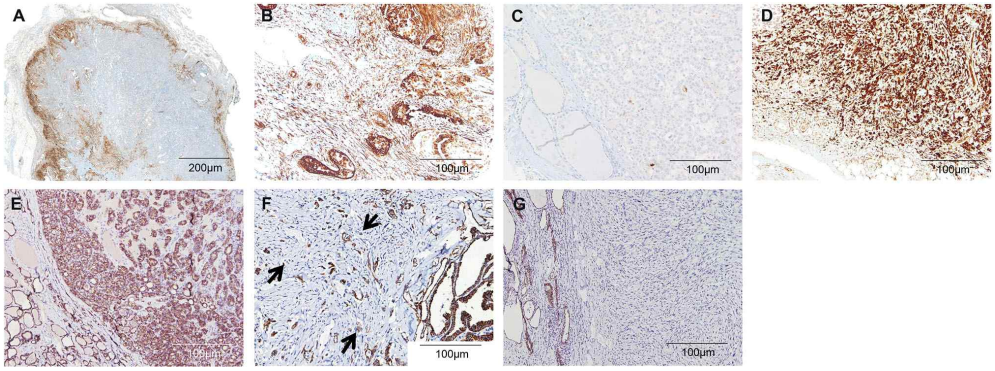

TUBB3 (A-D). A low power view of cPTC revealed TUBB3-positive tumor cells located at the invasive margin (A). A high power view of cPTC showed strong TUBB3 expression in both stromal cells and tumor cells at the invasive front (B). In EFVPTC, only a few scattered TUBB3-positive tumor cells were observed. Stromal cells were negative for TUBB3 in this case (C). Tumor cells of ATC were strongly positive for TUBB3 in diffuse pattern (D). E-cadherin (E-G). Tumor cells in EFVPTC generally maintained membranous E-cadherin expression (E). In cPTC, some tumor cells at the periphery showed loss of E-cadherin expression while tumor cells at the center retained membranous E-cadherin expression (F). ATC tumor cells showed loss of E-cadherin expression throughout the tumor (G).

Figure 2. Difference of TUBB3 and E-cadherin expression, and tumor budding among thyroid cancers

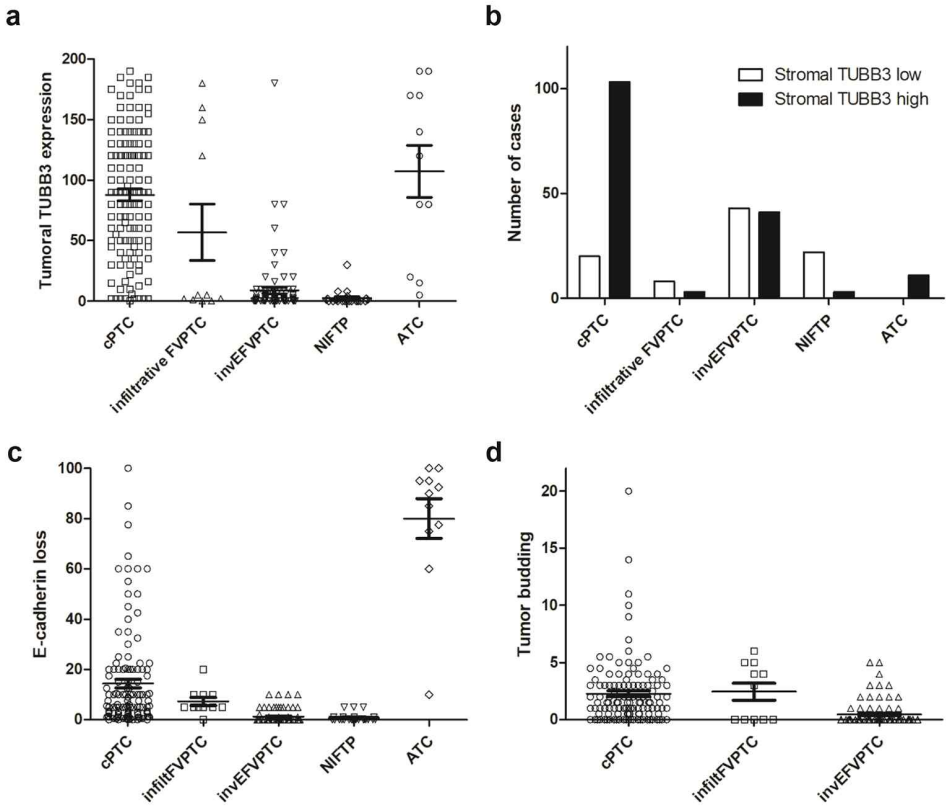

Tumoral TUBB3 expression (H-score) was highest in ATC, followed by cPTC, infiltrative FVPTC, invEFVPTC, and NIFTP (A). High stromal TUBB3 expression was more common in cPTC and ATC than in invEFVPTC and NIFTP (B). The proportion of tumor cells showing loss of E-cadherin expression was also highest in ATC, followed by cPTC, infiltrative FVPTC, invEFVPTC, and NIFTP (C). Tumor budding was more commonly observed in cPTC and infiltrative FVPTC than in EFVPTC (D).

Table 3. Statistical analysis in TUBB3 and E-cadherin expression and tumor budding among thyroid cancers

Parameters	ATC vs. cPTC	ATC vs. infiltrativeFVPTC	ATC vs. invEFVPTC	ATC vs. NIFTP	cPTC vs. infiltrativeFVPTC	cPTC vs. invEFVPTC	cPTC vs. NIFTP
Tumoral TUBB3†	1.000	0.400	<0.001*	<0.001*	0.650	<0.001*	<0.001*
Stromal TUBB3	1.000	1.000	0.010*	<0.001*	1.000	<0.001*	<0.001*
E-cadherin loss	<0.001*	<0.001*	<0.001*	<0.001*	1.000	<0.001*	<0.001*
Presence of TB	NA	NA	NA	NA	1.000	<0.001*	<0.001*
Number of TB	NA	NA	NA	NA	1.000	<0.001*	<0.001*

Table 3. continued.

Parameters	Infiltrative FVPTC vs invEFVPTC	Infiltrative FVPTC vs NIFTP	invEFVPTC vs NIFTP
Tumoral TUBB3†	0.480	0.010*	0.900
Stromal TUBB3	1.000	1.000	0.010*
E-cadherin loss	<0.001*	0.090	1.000
Presence of TB	0.220	<0.001*	0.110
Number of TB	0.020*	0.010*	0.150

†Tumoral TUBB3 in H-score.

*Statistically significant.

ATC, anaplastic thyroid carcinoma; cPTC, conventional papillary thyroid carcinoma; FVPTC, follicular variant papillary thyroid carcinoma; invEFVPTC, invasive encapsulated follicular variant papillary thyroid carcinoma; NIFTP, non-invasive follicular thyroid neoplasm with papillary-like nuclear feature; TB, tumor budding.

Tumor budding showed strong TUBB3 expression and was frequent in cPTCs and infiltrative FVPTCs (**Figure 3**). In cPTCs, a total of 97 out of 123 cases (78.9%) had tumor budding, whereas 6 infiltrative FVPTCs (54.5%) and 17 invasive EFVPTCs (20.2%) showed budding (**Table 2**). None of the NIFTP cases harbored these structures. Moreover, the number of cases showing tumor buddings, and the number of tumor buddings was higher in cPTCs and infiltrative FVPTCs than in invEFVPTCs (all $p<0.05$) (**Table 2-3, Figure 2**).

Figure 3. Tumor budding in conventional papillary carcinoma

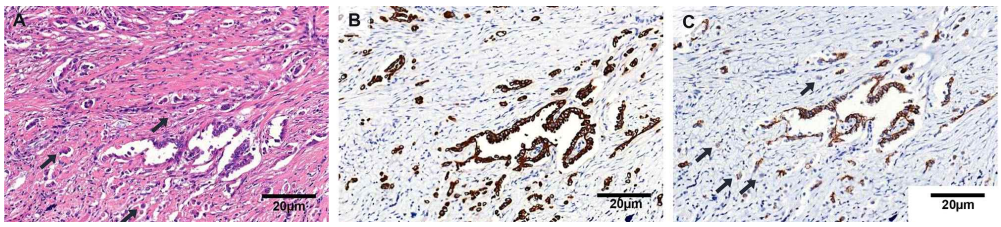

A high magnification view showed conventional papillary carcinoma with a single tumor cell or small clusters of tumor cells in fibrotic stroma at the invasive margin (x400) (A). These tumor budding were positive for cytokeratin immunohistochemistry (x400) (B). Membranous E-cadherin expression was lost in some of these cells (x400) (C).

The results of western blot and RT-PCR were concordant with those of IHC. The protein and mRNA expression of TUBB3 was highest in ATC cells (BHT101 and 8505C) and lowest in normal follicular cells (Htori-3). The cPTC (BCPAP) and FVPTC (MDA-T68) cells showed intermediate levels of protein and mRNA expression. IF study revealed evident EMT-related morphological changes, including loosening of cell contacts, and acquisition of spindle-shape, in TUBB3-positive cells (**Figure 4**)[51].

Figure 4. Western blot and RT-PCR in normal thyroid cells and thyroid cancer cells at baseline

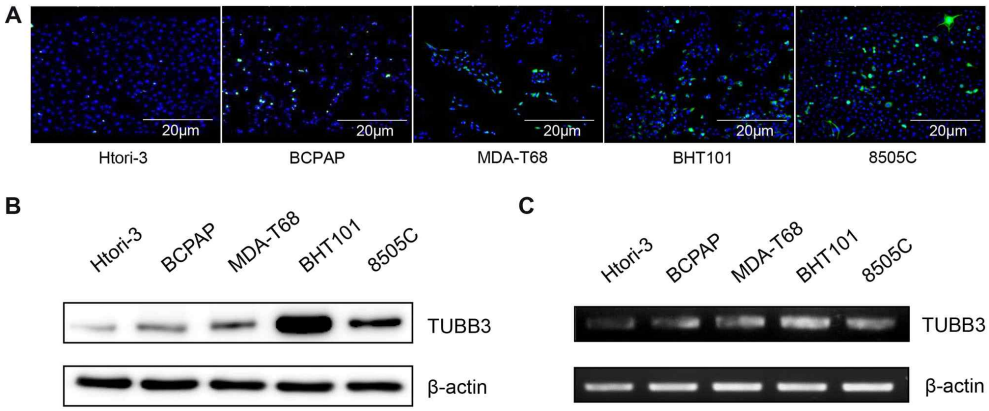

Immunofluorescent study revealed abundant TUBB3 (green) positive cells in ATC cells. TUBB3-positive cells showed spindle shape, suggestive of epithelial mesenchymal transition (A). Western blot (B) and RT-PCR (C) revealed higher TUBB3 expression in ATC than in cPTC and FVPTC.

3.3. TUBB3 was upregulated during stromal invasion

After the transwell invasion assay, only ATC cells (BHT101 and 8505C) managed to permeate the Matrigel and successfully reached the bottom membrane. The protein levels of TUBB3 and vimentin were increased in the bottom chamber cells compared with the baseline levels, while the protein expression of ECAD decreased after invasion. TUBB3 mRNA levels also increased after invasion. These phenomena were reversely validated after shRNA-mediated downregulation of TUBB3 in ATC cells (BHT101 and 8505C). After transfection with TUBB3 shRNA, fewer cells invaded through the Matrigel, and both ATC cells showed significantly decreased vimentin and TUBB3 protein levels, and increased ECAD levels. Likewise, TUBB3 mRNA levels decreased after shRNA transfection. The morphology of ATC cells before shRNA transfection showed spindled to polygonal shape, whereas the cells were round to oval shape after shRNA transfection (**Figure 5**).

Figure 5. Transwell invasion assay and shRNA transfection

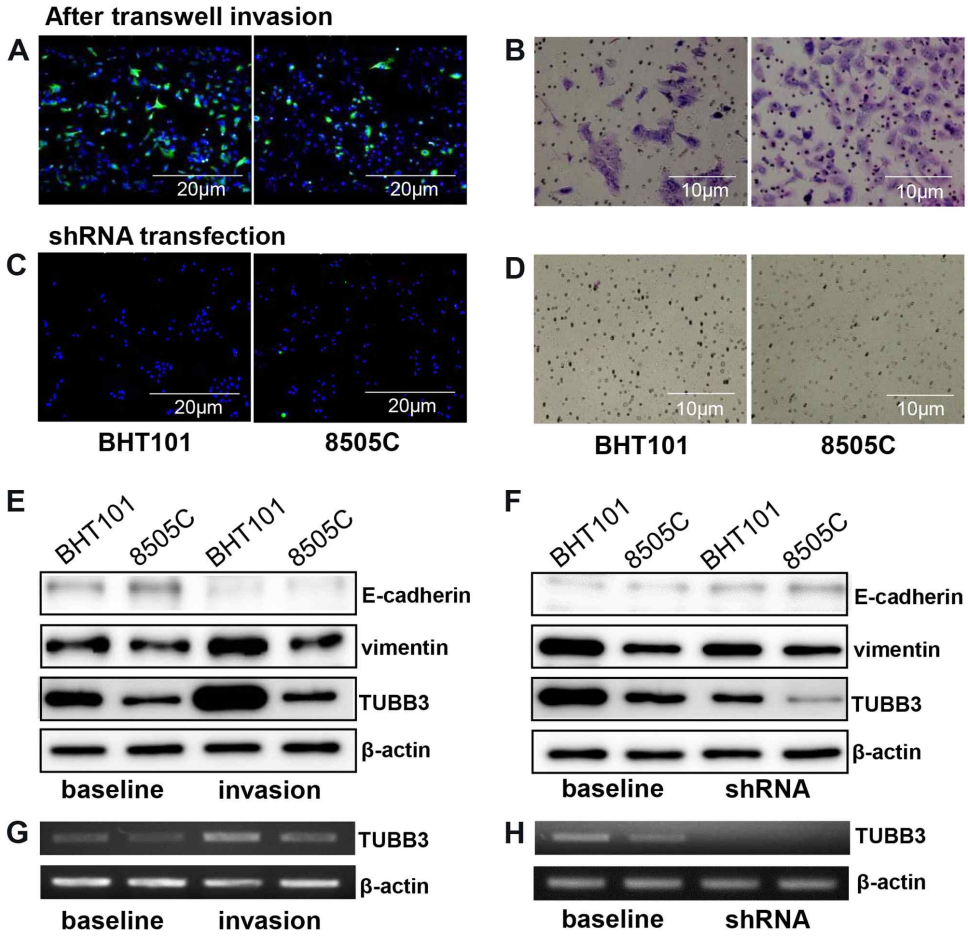

Immunofluorescent (A, C) and giemsa staining (B, D) revealed reduced invasion activity of ATC cells after shRNA transfection. Western blot revealed increased vimentin and TUBB3 protein levels and decreased E-cadherin protein levels after transwell invasion compared with baseline (E). RT-PCR also revealed increased TUBB3 mRNA levels after transwell invasion (G). Western blot after shRNA transfection showed decreased vimentin and TUBB3 protein levels, and increased E-cadherin protein levels compared with baseline (F). RT-PCR also revealed decreased TUBB3 mRNA expression after shRNA transfection (H).

Clinicopathological correlation and survival analysis

In cPTCs, higher tumoral TUBB3 H-score was associated with strong stromal TUBB3 expression, higher tumor budding, and positivity for BRAF mutation-specific antibody (all $p<0.05$). Additionally, higher tumoral TUBB3 H-score was associated with male gender, age over 55 years (all $p<0.05$), and more frequent disease progression ($p=0.005$). The loss of ECAD was associated with higher tumor budding and positivity for BRAF mutation-specific antibody (all $p<0.05$). Higher tumor budding was associated with BRAF positivity, age over 55 years, lymph node metastasis, advanced AJCC stage and disease progression (all $p<0.05$).

To evaluate the prognostic significance of various parameters, including tumoral TUBB3 H-score, cases were divided into two groups based on the cut-off value calculated by a receiver operator characteristic (ROC) curve. In univariate analysis, higher tumoral TUBB3 H-score (cutoff: 105, the area under the ROC curve, 0.67) and higher tumor budding (cutoff: 1.75, the area under the ROC curve, 0.63) were associated with inferior progression-free survival (PFS) (both $p<0.05$) (**Figure 6**). In multivariate analysis, distant metastasis ($p=0.002$), higher tumor budding ($p=0.004$) and higher tumoral TUBB3 H-score ($p=0.015$) remained independent prognostic factors for inferior PFS. Meanwhile, only high stage (1 versus 2-4) remained an independent prognostic factor for inferior OS ($p=0.001$) (**Table 3**).

In invasive EFVPTCs, loss of ECAD was associated with lymph node metastasis ($p=0.045$). In infiltrative FVPTCs,

NIFTPs and ATCs, the expression of TUBB3 and ECAD did not show any association with clinicopathologic parameters.

Figure 6. Kaplan-Meier analysis of patients based on tumoral TUBB3 expression (H-score) and tumor budding

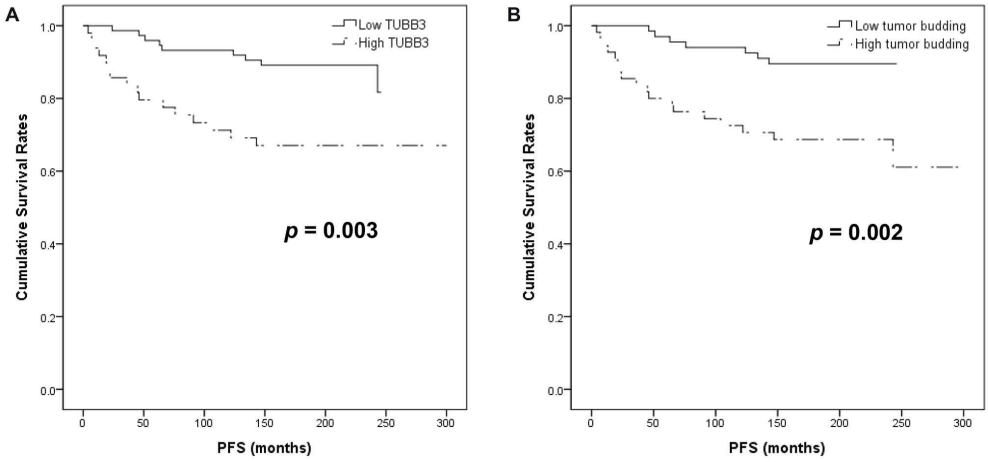

Higher tumoral TUBB3 H-score (A) and tumor budding (B) were associated with shorter progression-free survival.

Table 4. Survival analysis in conventional papillary thyroid carcinoma

Parameters	Univariate analysis (OS)		Multivariate analysis (OS)		Univariate analysis (PFS)		Multivariate analysis (PFS)
	OR (95% CI)	P-value	OR (95% CI)	P-value	OR (95% CI)	P-value	OR (95% CI)
Age > 55yrs	3.182 (1.066 – 9.501)	0.038*	–	NS	1.190 (0.587 – 2.409)	0.630	
Sex	0.650 (0.207 – 2.042)	0.461			0.450 (0.218 – 0.928)	0.031*	–
BRAF	0.790 (0.281 – 2.223)	0.655			0.668 (0.325 – 1.371)	0.271	
LN metastasis	0.616 (0.174 – 2.183)	0.453			1.686 (0.840 – 3.384)	0.142	
Distant metastasis	10.026 (2.121 – 47.386)	0.004*	–	NS	4.536 (1.749 – 11.767)	0.002*	4.939 (1.824 – 13.371)
Gross ETE	3.112 (1.107 – 8.744)	0.031*	–	NS	1.046 (0.430 – 2.541)	0.921	
Stage (1 vs 2-4)	7.925 (2.522 – 24.908)	<0.001*	7.115 (2.230 – 22.702)	0.001*	2.627 (1.311 – 5.262)	0.006*	–
Tumoral TUBB3†	2.233 (0.746 – 6.682)	0.151			3.545 (1.743 – 7.210)	<0.001*	2.690 (1.211 – 5.972)
Stromal TUBB3	1.490 (0.413 – 5.376)	0.543			2.276 (0.870 – 5.952)	0.094	
E-cadherin loss	0.588 (0.156 – 2.217)	0.433			1.696 (0.808 – 3.5559)	0.162	
Tumor budding	3.012 (0.779 – 11.650)	0.093			5.659 (2.528 – 12.672)	<0.001*	3.903 (1.549 – 9.838)

†Tumoral TUBB3 in H-score.

*Statistically significant.

OS, overall survival; PFS, progression-free survival; OR, odds ratio; CI, confidence interval; NS, not statistically significant; ETE, extrathyroidal extension.

TCGA data analysis

The TUBB3 mRNA level was highest in tall cell variant PTCs (log2-transformed counts of 9.3 ± 1.5), followed by cPTCs (log2-transformed counts of 8.6 ± 1.7) and FVPTCs (log2-transformed counts of 7.7 ± 2.0) (all $p<0.05$) (**Figure 7A**). The differences in ECAD, and vimentin among the above variants were not statistically significant (**Figure 8**). However, higher TUBB3 mRNA expression correlated with a higher EMT score (Pearson's $r=0.397$, $p<0.001$) (**Figure 7B**). The correlation coefficients between 17 genes, including TUBB3 and 16 EMT-related genes, are shown in **Figure 9**. Additionally, higher TUBB3 mRNA expression was correlated with higher vimentin ($p=0.049$) and the presence of BRAF V600E mutation ($p<0.001$). The Kaplan-Meier survival analysis showed that the patients with higher TUBB3 mRNA expression had shorter PFS than patients with lower TUBB3 mRNA expression ($p=0.041$) (**Figure 7**).

Figure 7. TUBB3 mRNA expression and its prognostic significance, and correlation with epithelial-mesenchymal transition (EMT) score (TCGA data)

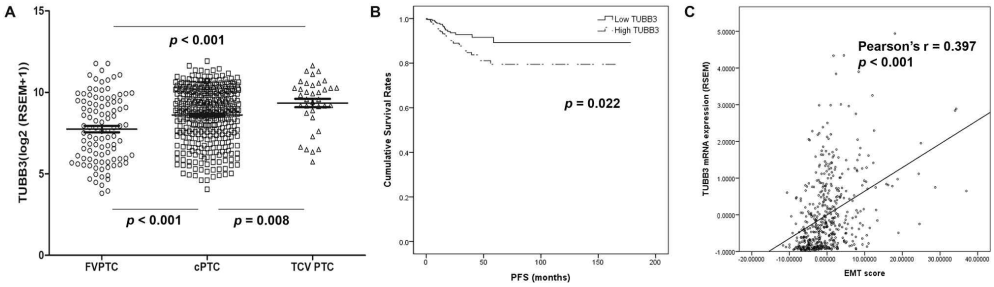

TUBB3 mRNA expression was highest in tall cell variant PTC, followed by cPTC and FVPTC (A). Patients with higher TUBB3 mRNA expression showed significantly shorter progression-free survival (B). TUBB3 mRNA expression was correlated with higher EMT score (C).

Figure 8. Differences in mRNA expression of E-cadherin and vimentin in papillary carcinoma (TCGA data)

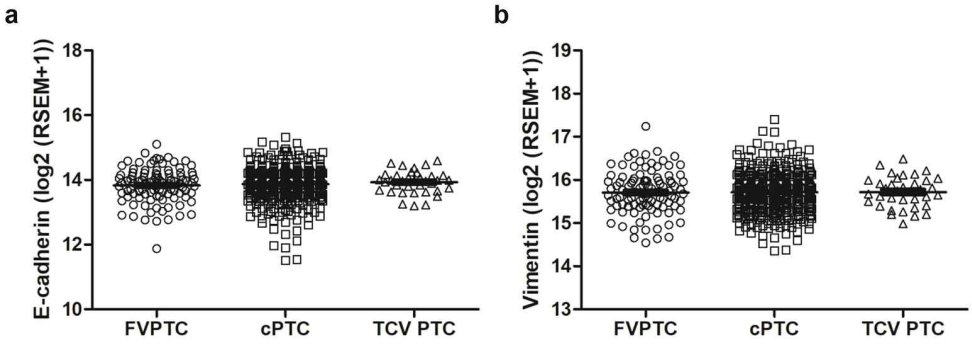

There were no differences in E-cadherin (A) and vimentin (B) mRNA expression levels among papillary carcinoma variants.

Figure 9. Correlation of mRNA levels among TUBB3 and EMT-related markers (TCGA data)

	TUBB3	VIM	CDH2	FOXC2	SNAI1	SNAI2	TWIST1	FN1	ITGB6	MMP2	MMP3	MMP9	SOX10	GSC	CDH1	DSP	OCLN
TUBB3	1.000	0.170*	-0.095	0.238*	0.088	0.321*	0.432*	0.804*	0.620*	0.482*	0.401	0.596	0.075	0.010	0.126*	0.351*	-0.155*
VIM	0.170*	1.000	0.088*	0.279*	0.267*	0.242*	0.255*	0.016	-0.052	0.312*	0.100*	0.096*	0.060	0.192*	0.022	-0.046	-0.068
CDH2	-0.095	0.088*	1.000	0.164*	0.171*	0.043	-0.011	-0.194*	-0.203*	0.003	-0.136*	-0.160*	0.074	0.04	-0.021	-0.077	0.038
FOXC2	0.238*	0.279*	0.164*	1.000	0.334*	0.556*	0.440*	0.222*	0.176*	0.495*	0.203*	0.205*	0.181*	0.231*	0.000	0.207*	0.143*
SNAI1	0.088	0.267*	0.171*	0.334*	1.000	0.368*	0.297*	-0.109*	0.098*	0.394*	0.125*	0.058	0.177*	0.245*	0.254*	0.012	-0.121*
SNAI2	0.321*	0.242*	0.043	0.556*	0.368*	1.000	0.711*	0.194*	0.218*	0.633*	0.381*	0.313*	0.230*	0.494*	-0.03	0.051	-0.122*
TWIST1	0.432*	0.255*	-0.011	0.440*	0.297*	0.711*	1.000	0.270*	0.250*	0.667*	0.506*	0.380*	0.136*	0.504*	-0.188*	-0.059	-0.288*
FN1	0.804*	0.016	-0.194*	0.222*	-0.109*	0.194*	0.270*	1.000	0.687*	0.353*	0.380*	0.528*	0.077	-0.203*	0.186*	0.585*	0.094*
ITGB6	0.620*	-0.052	-0.203*	0.176*	0.098*	0.218*	0.250*	0.687*	1.000	0.325*	0.389*	0.404*	0.053	-0.112*	0.328*	0.568*	0.146*
MMP2	0.482*	0.312*	0.003	0.495*	0.394*	0.633*	0.667*	0.353*	0.325*	1.000	0.501*	0.342*	0.174*	0.346*	-0.044	-0.108*	-0.173*
MMP3	0.401*	0.100*	-0.136*	0.203*	0.125*	0.381*	0.506*	0.380*	0.389*	0.501*	1.000	0.304*	0.059	0.146*	0.008	0.209*	-0.022
MMP9	0.596*	0.096*	-0.160*	0.205*	0.058	0.313*	0.380*	0.528*	0.404*	0.342*	0.304*	1.000	0.129*	0.125*	-0.055	0.175*	-0.193*
SOX10	0.075	0.060	0.074	0.181	0.177	0.23	0.136*	0.077	0.053	0.174*	0.059	0.129*	1.000	0.124*	0.059	0.038	0.049
GSC	0.010	0.192*	0.04	0.231*	0.245*	0.494*	0.504	-0.203	-0.112	0.346	0.146	0.125	0.124	1.000	-0.241	-0.318	-0.345
CDH1	0.126*	0.022	-0.021	0	0.254*	-0.030	-0.188*	0.186*	0.328*	-0.044	0.008	-0.055	0.059	-0.241*	1.000	0.587*	0.335*
DSP	0.351*	-0.046	-0.077	0.207*	0.012	0.051	-0.059	0.585*	0.568*	-0.108*	0.209*	0.175*	0.038	-0.318*	0.587*	1.000	0.472*
OCLN	-0.155	-0.068	0.038	0.143*	-0.121*	-0.122*	-0.288*	0.094*	0.146*	-0.173*	-0.022	-0.193*	0.049	-0.345*	0.335*	0.472*	1.000

1.0
0
-1.0

Correlation among TUBB3 and other EMT-related markers' mRNA expression levels are plotted as above.

Discussion

We suggest that overexpression of TUBB3 can be induced during stromal invasion of thyroid carcinoma and is associated with EMT. In our study, TUBB3 was expressed in tumor cells and the stroma of the invasive front, and upregulation of TUBB3 was observed during Matrigel penetration and was associated with an EMT-associated cellular morphology. High tumoral TUBB3 expression along with the presence of tumor budding was a negative prognostic factor in cPTC. These results support that TUBB3 is a new biomarker predicting adverse outcomes in thyroid carcinoma.

Although TUBB3 expression was believed to be exclusive in terminally differentiated neuroal and testis tissue and tumors originated from these tissues [18, 19], a number of researchers have demonstrated TUBB3 expression in epithelial tumors and focused on the role of TUBB3 regarding the resistance to taxane-based chemotherapy [21-23]. Later on, the prognostic significance of TUBB3 regardless of taxane-based chemotherapy was revealed [24-30, 52-55]. TUBB3 expression was proven as an indicator of tumor progression and aggressive behavior in various tumors, including thymic epithelial tumors, lung cancer, breast cancer, and colorectal cancer [24-30]; however, others reported that high TUBB3 expression was associated with a superior response to the drugs in breast and ovarian cancer [52-55]. These findings indicate that TUBB3 expression might be regulated in a complicated pattern and affect tumor progression in context-dependent way, which is influenced by

various biological factors or microenvironments of different organs.

Very few attempts have been made to investigate TUBB3 expression and its prognostic impact in thyroid cancer. In ATC, TUBB3 expression was associated with the resistance to taxane-based chemotherpay [44]. More recently, Colato et al. demonstrated in their preliminary reports that strong TUBB3 expression was observed in the invasive margin of PTCs with infiltrative growth pattern, while normal follicular cells, follicular adenomas, and PTCs with well demarcated margin were negative for TUBB3 [41, 42]. Similarly, the association between high TUBB3 expression and aggressive histologic features, including tall cell variant, squamous cell carcinoma or ATC components, angioinvasion, and disease recurrence, was revealed by Ciobanu et al [43]. In line with these previous studies, TUBB3 expression was predominantly higher in ATCs than in PTCs. Less aggressive tumors, including EFVPTCs and NIFTP, showed lower expression of TUBB3 than cPTCs and infiltrative FVPTCs. Validation of public data also consistently revealed higher TUBB3 mRNA expression in tall cell variant PTC than cPTCs and FVPTCs. TUBB3 expression in cPTCs was associated with disease progression but not death in both our cohort and public data. This might be related to the overall indolent behavior of cPTC showing low frequency of death (8.1% in our cohort, and 4.2% in public data). Nevertheless, considering that AJCC/TNM staging is based on predicting death, not recur or progression [11], TUBB3 can be a useful marker in that it can predict disease progression. Of note, TUBB3 was more frequently expressed in infiltrative FVPTCs than EFVPTCs or NIFTPs,

which suggests that TUBB3 can be used as a diagnostic marker in these follicular-patterned tumors with ambiguous histologic features.

In carcinoma, tumor cells at the invasive margin commonly undergo EMT process, during which epithelial tumor cells lose polarity and cell-cell adhesion, and acquire a mesenchymal phenotype [56]. EMT is considered critical for the initial steps of metastasis by enabling cells to gain motility and invasive potential [57], and the role of TUBB3 in the EMT process has yet to be uncovered. TUBB3 is a component of microtubule which contributes to cell motility by generating protrusive force via interaction with actin filaments [58, 59]. Previous studies demonstrated that TUBB3 expression can promote invasion and distant metastasis in breast cancer and colorectal cancer cells [60-62]. In breast cancer, SOX11, an embryonic mammarian epithelial cell marker, which is normally silenced before the birth, induced TUBB3 and other EMT-associated markers, and was associated with increased invasive and metastatic potential [61]. Liang et al. also demonstrated that long non-coding RNA (LncRNA) RPPH1 promoted invasion and metastasis or colon cancer cells via interacting with TUBB3 [62]. By binding to TUBB3, LncRNA inhibits ubiquitination of TUBB3 [62]. They additionally demonstrated that increased LncRNA led to upregulation of TUBB3 and Snail [62]. Others have also proved that upregulation of TUBB3 induced Snail pathway activation [40]. Our analyses of TCGA data also revealed a correlation between TUBB3 mRNA expression and EMT score, supporting previous studies. In our study, we observed EMT-related morphological

changes, including tumor budding, in TUBB3-positive cells and found that migration and invasion were more active in thyroid cancer cells with high TUBB3 expression. Tumor budding not only is considered a morphologic presentation of EMT [63, 64], but also has been validated as an important prognostic factor, even in early-stage colon cancer [36, 65, 66]. Similar to these studies, we found that increased tumor budding was associated with advanced disease status and poor outcome in cPTC. Although, the exact mechanism how TUBB3 induces Snail is yet to be uncovered, these previous studies and our results provide theoretical background for the claim that TUBB3 is activated through EMT and is a new prognostic biomarker.

The mechanism of TUBB3 activation has not been clearly elucidated, and various biological factors can be hypothesized to play a role. Hypoxia [67], and poor nutritional status, such as hypoglycemia [68], have been suggested as important causes of enhanced TUBB3 expression [68]. These two phenomena are commonly seen in the peripheral areas of tumors, and lead to genomic changes in cancer cells that can overcome the hostile microenvironment and induce cancer stem cell (CSC) characteristics [69]. Both hypoxia [70-72] and CSC features [73, 74] are closely related to the EMT process. TUBB3 is considered a marker of CSCs because it is enriched in CSCs and induces multidrug resistance in coordination with ABC transporters [75, 76]. These findings might explain why TUBB3 is selectively expressed in the peripheral part and invasive front of tumors and is associated with aggressive features in TUBB3 positive thyroid cancer.

In our study, TUBB3 was expressed not only in the tumor cells but also in the neighboring stroma. This suggests that microenvironmental factors that induce TUBB3 expression in tumor cells might also function in a similar way in stromal cells. Hypoxia contributes to the transformation of cancer-associated fibroblasts (CAFs), which encourage tumor growth and invasion to maintain stemness [69]. The source of TUBB3 in CAFs might be cancer cells, with paracrine regulation, and these CAFs are believed to participate in angiogenesis, tumor growth and progression [77, 78]. TUBB3 expression in thyroid carcinoma might occur with a tight connection with certain environmental stimuli and stromal interactions.

High TUBB3 expression in thyroid cancer cells correlated with positivity to BRAF mutation-specific antibody. This finding coincides with the public data from cBioPortal, which revealed a correlation between TUBB3 mRNA expression and BRAF V600E mutation. However, considering that the great majority of cPTCs in Koreans harbor BRAF mutations [79] and virtually no BRAF mutations are found in NIFTPs or EFVPTCs [80], this might be an indirect result without causality. High TUBB3 expression was associated with KRAS mutation and activated KRAS pathway in non-small cell lung cancer [81]. SiRNA blocking of KRAS resulted in decreased TUBB3 expression, suggesting TUBB3 is target of KRAS signaling pathway, thereby leading to tumor progression [81]. However, the association between TUBB3 expression and RAS or RAF signaling pathway in thyroid cancer is largely unknown. In this retrospective study, investigation of KRAS mutation in old archival blocks was limited, therefore it may be considered in further studies.

In conclusion, the present study is so far the first to show the role of TUBB3 in the pathogenesis of thyroid cancer. Our study indicates that TUBB3 plays a role in tumor progression via EMT. TUBB3 could be a novel prognostic marker as well as a potential druggable target in PTC.

Bibliography

1. Ahn HS, Kim HJ, Welch HG. Korea's thyroid-cancer "epidemic"-screening and overdiagnosis. N Engl J Med. 2014;371(19):1765-7.
2. Park S, Oh CM, Cho H, Lee JY, Jung KW, Jun JK, et al. Association between screening and the thyroid cancer "epidemic" in South Korea: evidence from a nationwide study. BMJ. 2016;355:i5745.
3. Haymart MR, Miller DC, Hawley ST. Active Surveillance for Low-Risk Cancers - A Viable Solution to Overtreatment? N Engl J Med. 2017;377(3):203-6.
4. Ito Y, Miyauchi A. Active Surveillance as First-Line Management of Papillary Microcarcinoma. Annu Rev Med. 2019;70:369-79.
5. Oh HS, Ha J, Kim HI, Kim TH, Kim WG, Lim DJ, et al. Active Surveillance of Low-Risk Papillary Thyroid Microcarcinoma: A Multi-Center Cohort Study in Korea. Thyroid. 2018;28(12):1587-94.
6. Ambrosi F, Righi A, Ricci C, Erickson LA, Lloyd RV, Asioli S. Hobnail Variant of Papillary Thyroid Carcinoma: a Literature Review. Endocr Pathol. 2017;28(4):293-301.
7. Kwon H, Oh HS, Kim M, Park S, Jeon MJ, Kim WG, et al. Active Surveillance for Patients With Papillary Thyroid Microcarcinoma: A Single Center's Experience in Korea. J Clin Endocrinol Metab. 2017;102(6):1917-25.
8. Nath MC, Erickson LA. Aggressive Variants of Papillary Thyroid Carcinoma: Hobnail, Tall Cell, Columnar, and Solid. Adv Anat Pathol. 2018;25(3):172-9.
9. Roman S, Sosa JA. Aggressive variants of papillary thyroid cancer. Curr Opin Oncol. 2013;25(1):33-8.

10. Siddiqui S, White MG, Antic T, Grogan RH, Angelos P, Kaplan EL, et al. Clinical and Pathologic Predictors of Lymph Node Metastasis and Recurrence in Papillary Thyroid Microcarcinoma. Thyroid. 2016;26(6):807-15.
11. Tuttle RM, Morris LF, Haugen B, Shah J, Sosa JA, Rohren E, et al. Thyroid-differentiated and anaplastic carcinoma. In: Amin MB, Edge SB, Greene F, Byrd D, Brookland RK, Washington MK, et al., editors. AJCC Cancer Staging Manual Eighth edition. 8th ed. New York: Springer International Publishing; 2017.
12. Byar DP, Green SB, Dor P, Williams ED, Colon J, van Gilse HA, et al. A prognostic index for thyroid carcinoma. A study of the E.O.R.T.C. Thyroid Cancer Cooperative Group. Eur J Cancer. 1979;15(8):1033-41.
13. Hay ID, Grant CS, Taylor WF, McConahey WM. Ipsilateral lobectomy versus bilateral lobar resection in papillary thyroid carcinoma: a retrospective analysis of surgical outcome using a novel prognostic scoring system. Surgery. 1987;102(6):1088-95.
14. Cady B, Rossi R. An expanded view of risk-group definition in differentiated thyroid carcinoma. Surgery. 1988;104(6):947-53.
15. American Thyroid Association Guidelines Taskforce on Thyroid N, Differentiated Thyroid C, Cooper DS, Doherty GM, Haugen BR, Kloos RT, et al. Revised American Thyroid Association management guidelines for patients with thyroid nodules and differentiated thyroid cancer. Thyroid. 2009;19(11):1167-214.
16. Haugen BR, Alexander EK, Bible KC, Doherty GM, Mandel SJ, Nikiforov YE, et al. 2015 American Thyroid Association Management Guidelines for Adult Patients with Thyroid Nodules and Differentiated Thyroid Cancer: The American Thyroid Association Guidelines Task Force on Thyroid Nodules and Differentiated Thyroid Cancer. Thyroid. 2016;26(1):1-133.
17. Mitchison T, Kirschner M. Dynamic instability of microtubule

growth. Nature. 1984;312(5991):237-42.

18. Lee MK, Rebhun LI, Frankfurter A. Posttranslational modification of class III beta-tubulin. Proc Natl Acad Sci U S A. 1990;87(18):7195-7199.

19. Lewis SA, Cowan NJ. Complex regulation and functional versatility of mammalian alpha- and beta-tubulin isotypes during the differentiation of testis and muscle cells. J Cell Biol. 1988;106(6):2023-2033.

20. Ferrandina G, Zannoni GF, Martinelli E, Paglia A, Gallotta V, Mozzetti S, et al. Class III beta-tubulin overexpression is a marker of poor clinical outcome in advanced ovarian cancer patients. Clin Cancer Res. 2006;12(9):2774-9.

21. Seve P, Isaac S, Tredan O, Souquet PJ, Pacheco Y, Perol M, et al. Expression of class III {beta}-tubulin is predictive of patient outcome in patients with non-small cell lung cancer receiving vinorelbine-based chemotherapy. Clin Cancer Res. 2005;11(15):5481-6.

22. Paradiso A, Mangia A, Chiriatti A, Tommasi S, Zito A, Latorre A, et al. Biomarkers predictive for clinical efficacy of taxol-based chemotherapy in advanced breast cancer. Ann Oncol. 2005;16 Suppl 4:iv14-9.

23. Lee KM, Cao D, Itami A, Pour PM, Hruban RH, Maitra A, et al. Class III beta-tubulin, a marker of resistance to paclitaxel, is overexpressed in pancreatic ductal adenocarcinoma and intraepithelial neoplasia. Histopathology. 2007;51(4):539-46.

24. Hoflmayer D, Ozturk E, Schroeder C, Hube-Magg C, Blessin NC, Simon R, et al. High expression of class III beta-tubulin in upper gastrointestinal cancer types. Oncol Lett. 2018;16(6):7139-45.

25. Kaira K, Serizawa M, Koh Y, Miura S, Kaira R, Abe M, et al. Expression of excision repair cross-complementation group 1, breast cancer susceptibility 1, and beta III-tubulin in thymic

epithelial tumors. J Thorac Oncol. 2011;6(3):606-13.
26. Koh Y, Jang B, Han SW, Kim TM, Oh DY, Lee SH, et al. Expression of class III beta-tubulin correlates with unfavorable survival outcome in patients with resected non-small cell lung cancer. J Thorac Oncol. 2010;5(3):320-5.
27. Lebok P, Ozturk M, Heilenkotter U, Jaenicke F, Muller V, Paluchowski P, et al. High levels of class III beta-tubulin expression are associated with aggressive tumor features in breast cancer. Oncol Lett. 2016;11(3):1987-94.
28. Portyanko A, Kovalev P, Gorgun J, Cherstvoy E. beta(III)-tubulin at the invasive margin of colorectal cancer: possible link to invasion. Virchows Arch. 2009;454(5):541-8.
29. Terry S, Ploussard G, Allory Y, Nicolaiew N, Boissiere-Michot F, Maille P, et al. Increased expression of class III beta-tubulin in castration-resistant human prostate cancer. Br J Cancer. 2009;101(6):951-6.
30. Zhao X, Yue C, Chen J, Tian C, Yang D, Xing L, et al. Class III beta-Tubulin in Colorectal Cancer: Tissue Distribution and Clinical Analysis of Chinese Patients. Med Sci Monit. 2016;22:3915-24.
31. Roche J. The Epithelial-to-Mesenchymal Transition in Cancer [published correction appears in Cancers (Basel). 2018 Mar 19;10(3):]. Cancers (Basel). 2018;10(2):52. Published 2018 Feb 16.
32. Nieto MA, Huang RY, Jackson RA, Thiery JP. EMT: 2016. Cell. 2016 Jun 30;166(1):21-45.
33. Roh MS, Lee JI, Choi PJ. Tumor budding as a useful prognostic marker in esophageal squamous cell carcinoma. Dis Esophagus. 2004;17(4):333-7.
34. Masugi Y, Yamazaki K, Hibi T, Aiura K, Kitagawa Y, Sakamoto M. Solitary cell infiltration is a novel indicator of poor prognosis and epithelial-mesenchymal transition in pancreatic

cancer. Hum Pathol. 2010 Aug;41(8):1061-8.

35. Yamaguchi Y, Ishii G, Kojima M, Yoh K, Otsuka H, Otaki Y, Aokage K, Yanagi S, Nagai K, Nishiwaki Y, Ochiai A. Histopathologic features of the tumor budding in adenocarcinoma of the lung: tumor budding as an index to predict the potential aggressiveness. J Thorac Oncol. 2010 Sep;5(9):1361-8.

36. Ueno H, Murphy J, Jass JR, Mochizuki H, Talbot IC. Tumour 'budding' as an index to estimate the potential of aggressiveness in rectal cancer. Histopathology. 2002;40(2):127-32.

37. Bronsert P, Enderle-Ammour K, Bader M, Timme S, Kuehs M, Csanadi A, Kayser G, Kohler I, Bausch D, Hoeppner J, Hopt UT, Keck T, Stickeler E, Passlick B, Schilling O, Reiss CP, Vashist Y, Brabletz T, Berger J, Lotz J, Olesch J, Werner M, Wellner UF. Cancer cell invasion and EMT marker expression: a three-dimensional study of the human cancer-host interface. J Pathol. 2014 Nov;234(3):410-22. doi: 10.1002/path.4416.

38. Wang HS, Liang WY, Lin TC, Chen WS, Jiang JK, Yang SH, Chang SC, Lin JK. Curative resection of T1 colorectal carcinoma: risk of lymph node metastasis and long-term prognosis. Dis Colon Rectum. 2005 Jun;48(6):1182-92.

39. Park KJ, Choi HJ, Roh MS, Kwon HC, Kim C. Intensity of tumor budding and its prognostic implications in invasive colon carcinoma. Dis Colon Rectum. 2005 Aug;48(8):1597-602.

40. Sobierajska K, Wieczorek K, Ciszewski WM, Sacewicz-Hofman I, Wawro ME, Wiktorska M, et al. beta-III tubulin modulates the behavior of Snail overexpressed during the epithelial-to-mesenchymal transition in colon cancer cells. Biochim Biophys Acta. 2016;1863(9):2221-33.

41. Colato C, Gobbato M, Dardano A, Brazzarola P, Monzani F, Chilosi M, et al. Class IIItubulin expression in papillary thyroid

carcinoma: an immunohistochemical assessment. 35th Annual Meeting of the European Thyroid Association Abstracts; Krakow, Poland2011. p. 128.

42. Colato C, Monzani F, Brazzarola P, Martignoni G, Chilosi M, Ferdeghini M. Immunohistochemical expression of [beta] III-tubulin and cell-cell adhesion proteins in papillary thyroid carcinoma: A preliminary report. Endocrine Abstracts. 2012;29:P1788.

43. Ciobanu DC, I-D.; Lozneanu, L.; Andriescu, E. C.; Leustean, L.; Giusca, S. E. Tubulin, a possible marker for the prognostic stratification and therapy in papillary thyroid carcinoma. Farmacia. 2018;66, 4:635-43.

44. Naoyoshi Onoda MH, Kennichi Kakudo, Atsuhiko Sakamoto, Kiminori Sugino, Noriaki Nakashima, Nobuyasu Suganuma, Shinichi Suzuki, Ken-ichi Ito, Iwao Sugitani. Factors Influencing the Chemo-Sensitivity of Weekly Paclitaxel for Anaplastic Thyroid Cancer: A Clinico-Pathologic Analysis of Cases Enrolled in a Clinical Trial. Journal of Thyroid Disorders and Therapy. 2019;8(1):231.

45. Nikiforov YE, Seethala RR, Tallini G, Baloch ZW, Basolo F, Thompson LD, Barletta JA, Wenig BM, Al Ghuzlan A, Kakudo K, Giordano TJ, Alves VA, Khanafshar E, Asa SL, El-Naggar AK, Gooding WE, Hodak SP, Lloyd RV, Maytal G, Mete O, Nikiforova MN, Nose V, Papotti M, Poller DN, Sadow PM, Tischler AS, Tuttle RM, Wall KB, LiVolsi VA, Randolph GW, Ghossein RA. Nomenclature Revision for Encapsulated Follicular Variant of Papillary Thyroid Carcinoma: A Paradigm Shift to Reduce Overtreatment of Indolent Tumors. JAMA Oncol. 2016 Aug 1;2(8):1023-9.

46. Lloyd RV, Osamura RY., Kloppel G., Rosai J. WHO Classification of Tumours of Endocrine Organs. 4th ed. France: Lyon; 2017.

47. Levallet G, Bergot E, Antoine M, Creveuil C, Santos AO,

Beau-Faller M, et al. High TUBB3 expression, an independent prognostic marker in patients with early non-small cell lung cancer treated by preoperative chemotherapy, is regulated by K-Ras signaling pathway. Mol Cancer Ther. 2012;11(5):1203-13.

48. Ghossein RA, Katabi N, Fagin JA. Immunohistochemical detection of mutated BRAF V600E supports the clonal origin of BRAF-induced thyroid cancers along the spectrum of disease progression. J Clin Endocrinol Metab. 2013;98(8):E1414-21.

49. Choe JY, Park M, Yun JY, Na HY, Go H, Kim HJ, et al. PELI1 expression is correlated with MYC and BCL6 expression and associated with poor prognosis in diffuse large B-cell lymphoma. Mod Pathol. 2016;29(11):1313-23.

50. Gibbons DL, Creighton CJ. Pan-cancer survey of epithelial-mesenchymal transition markers across the Cancer Genome Atlas. Dev Dyn. 2018;247(3):555-64.

51. Lee JM, Dedhar S, Kalluri R, Thompson EW. The epithelial-mesenchymal transition: new insights in signaling, development, and disease. J Cell Biol. 2006;172(7):973-81.

52. Galmarini CM, Treilleux I, Cardoso F, Bernard-Marty C, Durbecq V, Gancberg D, et al. Class III beta-tubulin isotype predicts response in advanced breast cancer patients randomly treated either with single-agent doxorubicin or docetaxel. Clin Cancer Res. 2008;14(14):4511-6.

53. Wang Y, Sparano JA, Fineberg S, Stead L, Sunkara J, Horwitz SB, et al. High expression of class III beta-tubulin predicts good response to neoadjuvant taxane and doxorubicin/cyclophosphamide-based chemotherapy in estrogen receptor-negative breast cancer. Clin Breast Cancer. 2013;13(2):103-8.

54. Akasaka K, Maesawa C, Shibazaki M, Maeda F, Takahashi K, Akasaka T, et al. Loss of class III beta-tubulin induced by

histone deacetylation is associated with chemosensitivity to paclitaxel in malignant melanoma cells. J Invest Dermatol. 2009;129(6):1516-26.

55. Aoki D, Oda Y, Hattori S, Taguchi K, Ohishi Y, Basaki Y, et al. Overexpression of class III beta-tubulin predicts good response to taxane-based chemotherapy in ovarian clear cell adenocarcinoma. Clin Cancer Res. 2009;15(4):1473-80.

56. Mittal V. Epithelial Mesenchymal Transition in Tumor Metastasis. Annu Rev Pathol. 2018;13:395-412.

57. Thiery JP, Acloque H, Huang RY, Nieto MA. Epithelial-mesenchymal transitions in development and disease. Cell. 2009;139(5):871-90.

58. Howard J, Hyman AA. Dynamics and mechanics of the microtubule plus end. Nature. 2003;422(6933):753-8.

59. Etienne-Manneville S, Hall A. Integrin-mediated activation of Cdc42 controls cell polarity in migrating astrocytes through PKCzeta. Cell. 2001;106(4):489-98.

60. Kanojia D, Morshed RA, Zhang L, et al. βIII-Tubulin Regulates Breast Cancer Metastases to the Brain. Mol Cancer Ther. 2015;14(5):1152-1161.

61. Oliemuller E, Newman R, Tsang SM, Foo S, Muirhead G, Noor F, Haider S, Aurrekoetxea-Rodr□guez I, Vivanco MD, Howard BA. SOX11 promotes epithelial/mesenchymal hybrid state and alters tropism of invasive breast cancer cells. Elife. 2020 Sep 10;9:e58374.

62. Liang ZX, Liu HS, Wang FW, Xiong L, Zhou C, Hu T, et al. LncRNA RPPH1 promotes colorectal cancer metastasis by interacting with TUBB3 and by promoting exosomes-mediated macrophage M2 polarization. Cell Death Dis. 2019;10(11):829.

63. Dawson H, Lugli A. Molecular and pathogenetic aspects of tumor budding in colorectal cancer. Front Med (Lausanne). 2015;2:11.

64. De Smedt L, Palmans S, Andel D, Govaere O, Boeckx B, Smeets D, et al. Expression profiling of budding cells in colorectal cancer reveals an EMT-like phenotype and molecular subtype switching. Br J Cancer. 2017;116(1):58-65.
65. Bosch SL, Teerenstra S, de Wilt JH, Cunningham C, Nagtegaal ID. Predicting lymph node metastasis in pT1 colorectal cancer: a systematic review of risk factors providing rationale for therapy decisions. Endoscopy. 2013;45(10):827-34.
66. Petrelli F, Pezzica E, Cabiddu M, Coinu A, Borgonovo K, Ghilardi M, et al. Tumour Budding and Survival in Stage II Colorectal Cancer: a Systematic Review and Pooled Analysis. J Gastrointest Cancer. 2015;46(3):212-8.
67. Katsetos CD, Del Valle L, Geddes JF, Assimakopoulou M, Legido A, Boyd JC, et al. Aberrant localization of the neuronal class III beta-tubulin in astrocytomas. Arch Pathol Lab Med. 2001;125(5):613-24.
68. Raspaglio G, De Maria I, Filippetti F, Martinelli E, Zannoni GF, Prislei S, et al. HuR regulates beta-tubulin isotype expression in ovarian cancer. Cancer Res. 2010;70(14):5891-900.
69. Lau EY, Ho NP, Lee TK. Cancer Stem Cells and Their Microenvironment: Biology and Therapeutic Implications. Stem Cells Int. 2017;2017:3714190.
70. Cho KH, Choi MJ, Jeong KJ, Kim JJ, Hwang MH, Shin SC, et al. A ROS/STAT3/HIF-1alpha signaling cascade mediates EGF-induced TWIST1 expression and prostate cancer cell invasion. Prostate. 2014;74(5):528-36.
71. Ide T, Kitajima Y, Miyoshi A, Ohtsuka T, Mitsuno M, Ohtaka K, et al. Tumor-stromal cell interaction under hypoxia increases the invasiveness of pancreatic cancer cells through the hepatocyte growth factor/c-Met pathway. Int J Cancer. 2006;119(12):2750-9.
72. Ren T, Zhang W, Liu X, Zhao H, Zhang J, Zhang J, et al.

Discoidin domain receptor 2 (DDR2) promotes breast cancer cell metastasis and the mechanism implicates epithelial-mesenchymal transition programme under hypoxia. J Pathol. 2014;234(4):526-37.

73. Mani SA, Guo W, Liao MJ, Eaton EN, Ayyanan A, Zhou AY, et al. The epithelial-mesenchymal transition generates cells with properties of stem cells. Cell. 2008;133(4):704-15.

74. Morel AP, Lievre M, Thomas C, Hinkal G, Ansieau S, Puisieux A. Generation of breast cancer stem cells through epithelial-mesenchymal transition. PLoS One. 2008;3(8):e2888.

75. Li W, Zhai B, Zhi H, Li Y, Jia L, Ding C, et al. Association of ABCB1, beta tubulin I, and III with multidrug resistance of MCF7/DOC subline from breast cancer cell line MCF7. Tumour Biol. 2014;35(9):8883-91.

76. Moitra K, Lou H, Dean M. Multidrug efflux pumps and cancer stem cells: insights into multidrug resistance and therapeutic development. Clin Pharmacol Ther. 2011;89(4):491-502.

77. Calon A, Tauriello DV, Batlle E. TGF-beta in CAF-mediated tumor growth and metastasis. Semin Cancer Biol. 2014;25:15-22.

78. Erdogan B, Webb DJ. Cancer-associated fibroblasts modulate growth factor signaling and extracellular matrix remodeling to regulate tumor metastasis. Biochem Soc Trans. 2017;45(1):229-36.

79. Lee SE, Hwang TS, Choi YL, Kim WY, Han HS, Lim SD, et al. Molecular Profiling of Papillary Thyroid Carcinoma in Korea with a High Prevalence of BRAF(V600E) Mutation. Thyroid. 2017;27(6):802-10.

80. Kim M, Jeon MJ, Oh HS, Park S, Kim TY, Shong YK, et al. BRAF and RAS Mutational Status in Noninvasive Follicular Thyroid Neoplasm with Papillary-Like Nuclear Features and Invasive Subtype of Encapsulated Follicular Variant of Papillary

Thyroid Carcinoma in Korea. Thyroid. 2018;28(4):504-10.

81. Levallet G, Bergot E, Antoine M, Creveuil C, Santos AO, Beau-Faller M, de Fraipont F, Brambilla E, Levallet J, Morin F, Westeel V, Wislez M, Quoix E, Debieuvre D, Dubois F, Rouquette I, Pujol JL, Moro-Sibilot D, Camonis J, Zalcman G; Intergroupe Francophone de Canc□rologie Thoracique (IFCT). High TUBB3 expression, an independent prognostic marker in patients with early non-small cell lung cancer treated by preoperative chemotherapy, is regulated by K-Ras signaling pathway. Mol Cancer Ther. 2012 May;11(5):1203-13.

국문 초록

갑상선암은 전세계적으로도 유병률이 높은 편으로, 최근 우리나라의 경우 고해상도 초음파의 발달과 함께 그 유병률이 가파르게 증가하였다. 대부분의 분화 갑상선암 환자의 경우 예후가 좋은 편이지만 일부에서는 국소재발이나 원격전이를 동반하는 공격적인 행동양식을 보이기 때문에 많은 연구자들이 갑상선암에서 질병의 진행을 예측할 수 있는 지표에 대해 연구해왔다. American Thyroid Association에서 2015년에 갑상선암 환자의 질병의 재발 위험도를 예측하는 시스템을 고안한 바 있으나, 아직 충분히 평가되지 않았으며 여전히 예후를 보다 정확하게 예측할 수 있는 새로운 바이오마커의 규명이 필요하다. 본 연구에서는 갑상선암에서 class III beta tubulin(TUBB3)이 종양의 침습성, 상피간엽이행 및 예후와 연관되어 있는지 알아보고 새로운 바이오마커로서의 가능성을 탐색하고자 하였다.

123례의 conventional type 유두암종, 11례의 침습성 여포변이 유두암종, 84례의 피막성 여포변이 유두암종, 25례의 유두암종유사핵모양비침습소포종양(noninvasive follicular thyroid neoplasm with papillary-like nuclear features)를 포함한 총 254례의 갑상선암의 조직에서 종양과 종양 주변 부위를 포함하도록 tissue microarray(TMA)를 제작하고 TUBB3, E-cadherin 면역조직화학염색을 시행하였다. 추가로, 종양 주변 부위에서 상피간엽이행과 연관된 암발아현상(tumor budding)을 계측하였다. 또, 갑상선 정상 여포 세포주(Htori-3), 유두암종 세포주(BCPAP), 유두암종의 여포성 변이 세포주(MDA-T68), 역분화암종 세포주(BHT101, 8505C)에서 기저 상태 및 shRNA를 이용한 트랜스펙션 전후로 transwell invasion assay의 결과와 TUBB3의 단백질 및 mRNA 발현량을 확인하고 세포주 간 차이를 분석하였다.

면역조직화학염색 결과, conventional type의 유두암종과 역분화암종에서 여포성 변이 유두암종, 유두암종유사핵모양비침습소포종양에

비해 TUBB3 발현률이 더 높고 E-cadherin의 발현률은 낮았으며, Conventional type 유두암종의 경우 TUBB3의 고발현과 암발아현상이 연관되어 있었다. 세포주 실험 결과 기저 상태에서 역분화암종 세포에서 TUBB3 단백질, mRNA 발현이 가장 높고 Transwell invasion assay 결과 이들 역분화암종 세포만 하실(lower chamber)로 침윤 가능하였다. shRNA 트랜스펙션을 통해 TUBB3 발현을 억제한 후에는 하실로 침윤하는 세포의 수가 현저히 감소하였다. 단변량 생존 분석에서 TUBB3 발현률이 높은 군과 암발아현상이 높은 군에서 그렇지 않은 군에 비해 무진행생존기간이 유의하게 짧았다. 이러한 결과는 공공데이터 포털인 cbioportal을 통해 얻은 TCGA 자료에서도 검증하였으며, 예후가 나쁜 큰키세포형 유두암종, conventional type 유두암종, 여포변이 유두암종 순서로 TUBB3 mRNA 발현량이 높았다. TUBB3 mRNA 발현량은 상피간엽이행과 연관된 16개의 마커를 조합하여 구성한 지표(EMT score)와 양의 상관관계를 보였다.

본 연구 결과, 갑상선암에서 TUBB3의 발현은 종양의 침습적인 성장과 연관이 있으며 이는 상피간엽이행과 관계가 있을 것으로 추정된다. 또한 conventional type 유두암종에서 TUBB3가 새로운 예후인자로 사용될 수 있을 것으로 판단된다.

주요어: 갑상선암, Class III beta-tubulin, 침윤, 상피간엽이행, 예후
학번: 2014-21977